Nuclear Mathematical and Computational Sciences: A Century in Review, A Century Anew
Gatlinburg, Tennessee, April 6-11, 2003, , American Nuclear Society, LaGrange Park, IL (2003)

COMPARATIVE ANALYSIS

OF PBMR CORE PHYSICS TEST PROBLEMS

B. Tyobeka and K. Ivanov
Nuclear Engineering Program
The Pennsylvania State University, USA
Bmt128@psu.edu; kni1@psu.edu

F. Reitsma
PBMR Pty, (Ltd) South Africa
Frederik.Reitsma@pbmr.co.za

D. Lee, and T. Downar
Department of Nuclear Engineering
Purdue University, USA
lee100@ecn.purdue.edu ; downar@ecn.purdue.edu

ABSTRACT

The Pebble Bed Modular Reactor (PBMR) configuration is one of the most promising reactor concepts for next generation power reactors, and thus has garnered substantial interest and research investment in the international nuclear community. Further development and maturation of this novel concept demands, among other things, verification of its safety features via reliable, high fidelity physics models and robust, efficient, and accurate computational tools. This has motivated the development of more accurate and efficient tools to analyze the neutronics behavior for the design and safety evaluations of the PBMR In addition to the development of new neutronics methods, this includes defining appropriate benchmarks to verify and validate the new methods in computer codes. This paper addresses the benchmarking of core simulation methods through a set of multi-dimensional computational test problems. The intention is to develop these test problems into HTGR benchmarks similar to the well-known IAEA PWR steady-state benchmarks. The benchmarks developed here were analyzed with three different codes: VSOP, NEM, and PARCS. The results obtained in this study have shown a reasonable agreement between the codes and has also shown that NEM, being a nodal expansion method's code has the capability to reproduce the results of the VSOP code at reasonable computational cost.

Key Words: benchmarks, PBMR, neutronics

1. INTRODUCTION

The Pebble-Bed Modular Reactor (PBMR) is a High-Temperature Gas-cooled Reactor (HTGR) concept, which has attracted the attention of the nuclear research and development community. The use of graphite as both moderator and structural material distinguishes the HTGR from other thermal reactor designs. It also eliminates the need for metal cladding and other structure material in the core assembly. Coated fuel particles in either prismatic or pebble-bed cores distinguish the HTGR from other graphite-moderated reactors such as the British Magnox and AGR (Advanced Gas-Cooled Reactor). Although very high coolant temperatures are normal (>900°C at the outlet of hot channels), the structural integrity of the particle coating keeps the fuel confined even under loss-of-flow or loss-of-pressure conditions. Heavy metal kernels of 0.5mm diameter mixed with graphite in either pebbles of fuel compacts means a tight coupling between the moderator and fuel and a resulting strong negative temperature feedback coefficient. The use of helium as coolant is also a unique feature. The chemical inertness and transparency to neutrons means that direct void reactivity feedback effects are negligible. The high coolant outlet temperatures make the HTGR a potential power source for process heat applications. The modular pebble-bed core consists of a cylindrical graphite vessel/reflector that contains upwards of 450,000 pebbles. Each fuel pebble contains between 10000 and 15000 particles for a total of, depending upon the design, seven to nine grams of uranium enriched to about 8% U-235. The pebbles are randomly packed in the vessel with a packing density between 0.59 and 0.64. Helium gas is blown in from the top and is forced through the packed bed to carry off heat. All these features make the modular pebble-bed High Temperature Gas-cooled Reactor a suitable candidate for Generation IV nuclear system. However, the deterministic neutronics methods available to design and analyze PBMRs have, in most cases, lagged behind the state of the art compared to other reactor technologies. This has motivated the development of more accurate and efficient tools to analyze the neutronics behavior for the design and safety evaluations of the PBMR. In addition to the implementation of new neutronics methods, this development includes defining appropriate benchmarks to verify and validate the new methods in computer codes. This paper addresses the benchmarking of core simulation methods through a set of multi-dimensional computational test problems. It is a joint effort between three institutions namely: Penn State University, Purdue University and the PBMR Company in South Africa. The ultimate intention is to develop these test problems into HTGR benchmarks similar to the well-known IAEA PWR steady-state benchmarks [1]. The test cases developed here were analyzed with three different codes: VSOP (PBMR Co), NEM (Penn State), and PARCS (Purdue).

2. MODELS FOR COMPUTATIONAL ANALYSIS

As mentioned above, Penn State, Purdue and the PBMR Co using three different computer codes and different calculational models but the same database performed the calculational work. A brief description of the codes used is given in the next subsections:

2.1 The VSOP Code

VSOP (Very Superior Old Programs) [2] developed many years ago in Germany with the HTGR program is a suite of codes presently used at the PBMR Company for the design and safety analysis of the PBMR. It consists of cross-section libraries and processing routines and neutron spectrum evaluation based upon the GAM and THERMOS codes, two-dimensional (2-D) and three-dimensional (3-D) diffusion, depletion routines, in-core and out-of-pile fuel management, fuel cycle cost analysis, and thermal hydraulics for pebble-bed reactors. Until recently, it was the only code generally available for life-cycle analysis of PBMRs. The diffusion module, based on the CITATION finite difference method, synthesizes the R-Z flux distribution in four energy groups from one-dimensional (axial) calculations For each CITATION

region the 4-group macroscopic cross sections are calculated by VSOP using the macroscopic cross sections from the applicable VSOP layers and by applying volume weighting. Note that the VSOP layer macroscopic cross sections are determined from the microscopic cross sections obtained from GAM and THERMOS (spectrum calculation) and the number densities (and volume fraction) of each batch of fuel in that layer. The CITATION composition mesh structure can further be refined (sub-divided) in order to obtain an accurate finite-difference diffusion solution. For HTR studies a choice of four energy groups have proven to be sufficient, i.e. a thermal energy group with energies between 0 to 1.86 eV, two epithermal groups with energies ranging from 1.86 to 29.0 eV and 29.0 and 1.11 MeV, and a fast energy group with energies between 1.11 and 10 MeV. No provision for up-scatters have been made in the current VSOP, and therefore limiting the user to a single thermal energy group. In the void above the pebble bed calculations are performed employing adapted diffusion coefficients. Since a diffusion coefficient for each coordinate direction has been implemented the different streaming effects (depending on the relative size and shape of the void) can be adjusted.

Forty isotopes can be tracked explicitly in up to 200 compositions and the spectrum calculation is repeated when a significant change in the spectrum is expected. The fuel management module tracks 'batches' of pebble from the moment of entry into the core, through recycling, and to eventual discharge. The batches are treated as though they reside in a stationary manner in assigned sections of fuel streamlines. After each time step, they are moved discontinuously to the next region in the streamline. The module simulates shuffling (recirculation) in this manner for currently known pebble-bed designs. It has been extended to include burnup-dependent optional re-loading of pebbles and different fuel streams. The time-dependent capability allows VSOP to model changes in the fueling scheme in mid-cycle. This code is widely accepted as the most appropriate suite of codes for the fuel management and safety analysis of pebble-bed reactors. Though effective for many situations, it is two generations of codes and methods older than the state of the art in neutronics solvers. In particular, this method is significantly slower than one that uses a nodal diffusion solver, and it is thus a less effective tool for frequent repetitive calculations needed for design and optimization.

2.2 The Nodal Expansion Method Code (NEM)

NEM [3] is a 3-D multi-group nodal diffusion code used at The Pennsylvania State University (PSU) for modeling both steady state and transient core conditions based on the nodal expansion method. This method for solving the nodal equations in three dimensions was developed by Finnemann [4]. It utilizes a transverse integration procedure and is based on the partial current formulation of the nodal balance equations. The leakage term in the one-dimensional transverse integrated equations is approximated by a standard parabolic expansion using the transverse leakages in three neighboring nodes. The nodal coupling relationships are expressed in partial current formulation and the time dependence of the neutron flux is approximated by a first order, fully explicit, finite difference scheme. This method has been shown to be very efficient although it lacked the precision of the advanced nodal codes. Recently an upgrade of the method has been completed, replacing the fourth order polynomial expansion with a semi-analytical expression utilizing a more accurate approximation of the transverse leakage. The code has options for modeling of 3-D Cartesian, cylindrical and hexagonal geometry. The cylindrical option utilizes fourth-order polynomial expansions of the 1-D transverse-integrated flux distribution in the R-, Z- and θ-directions. The cylindrical option has been verified using the Dodd's benchmark problem [1]. It is important to note that the detailed treatment of the effects of azimuthally dependent reactor control rods requires a full three-dimensional representation of the PBMR and it is possible to model that with NEM. Work is currently underway at Penn State to include the option of modeling the cone at the bottom of the pebble-bed leading to the de-fueling chute and to also implement the modeling of directional diffusion coefficients [5] to account for the anisotropy of the flux in the void regions of the core for example, at the top of the pebble-bed.

2.3 The Purdue Advanced Reactor Core Simulator (PARCS)

PARCS (Purdue Advanced Reactor Core Simulator) [6] is the U.S. NRC neutronics code used for core simulation and solves the multi-group, steady state and time-dependent neutron diffusion equation in 3-D Cartesian, hexagonal, and cylindrical geometries. For Cartesian coordinate, multi-group SP_3 transport kernel is also available. The *coarse mesh finite difference* (CMFD) formulation is employed in PARCS to solve for the neutron fluxes in the homogenized nodes. In rectangular geometry, the *analytic nodal method* (ANM) is used to solve the two-node problems for accurate resolution of coupling between nodes in the core, whereas the *triangle-based polynomial expansion nodal* (TPEN) method is used for the same purpose in hexagonal geometry. For cylindrical geometry, non-linear CMFD with one-node local solution is implemented to solve multi-group, 3-D diffusion equation. A depletion capability has also recently been added to PARCS, which includes cross section interface capability to lattice physics codes such as HELIOS. PARCS has been coupled to the U.S. NRC thermal-hydraulics codes RELAP5 and TRAC-M and has been verified using a suite of OECD benchmark problems. The results presented in this paper are used to verify the performance of a recently implemented multi-group FMFD (Fine Mesh Finite Difference) R-Z-θ kernel in PARCS.

3. BENCHMARK DESCRIPTION

Three PBMR core physics benchmark problems were defined for deterministic neutronics methods validation [7]. The first two problems represent a simplified model of an HTGR operating on an once through then out (OTTO) fuelling scheme, whereas the third problem is a realistic 268 MWt PBMR core model operating on a multi-pass fuelling scheme. For each of the benchmark problems, four group cross sections and scattering matrices data are provided as a part of benchmark specifications. They were generated with the VSOP code for an equilibrium core and with given temperatures (no thermal hydraulic calculations performed). The broad group energy boundaries, fission source distribution and energy release per fission are defined below.

3.1 Geometric and Material Description of Test Case 1

Test case 1 is a simplified cylindrical reactor with a fuel diameter of 200 cm and a side reflector with a total thickness of 100 cm. The core total height is 518 cm with a fuel height of 318 cm and top and bottom reflectors of 100 cm each. Provision has been made in the side reflector to insert a ring of control absorber material. This area, with a thickness of 13 cm is located at a distance of 6 cm from the active core within the side reflector. An OTTO cycle was assumed and the active core was divided into ten equally sized axial material layers. A single material mesh is assumed for the total active fuel radius and thus no burn-up or material variation is assumed in the radial direction. The material composition-numbering scheme is shown in Figure 1. A zero net current boundary condition is applied on the central axis while zero flux boundary conditions are applied to all of the other boundaries beyond the graphite reflector. The dimensions (in cm) are as follows: in radial direction the radii (from the center to outside) are: 0.0, 100.0, 106.0, 119.0, and 200.0; in axial direction (from bottom to top) the height is: 0.0, 100.0, 131.8, 163.6, 195.4, 227.2, 259.0, 290.8, 322.6, 354.4, 386.2, 418.0, and 518.0. The total volume of active core is 9.9903 m^3 and a power of 10 MW is used for flux normalization. In this first test case the 4-group cross sections for all the material regions are provided. However, since no control rods are inserted (in the first case), the cross sections of regions 14-24 are identical as shown in Figure 1 below. In the test

case 2 the same geometrical and material numbering system will be used to assign different (absorber material) properties to these regions. The cross sections and scattering matrices data were generated using the VSOP code and can be availed to interested participants. The broad group energy boundaries, fission source distribution and energy release per fission are defined as follows:

BROAD GROUP ENERGY BOUNDARIES (eV):
0.10000000E+08; 0.11108996E+06; 0.29023203E+02; 0.18553914E+01.

FISSION SOURCE DISTRIBUTION:
0.98439 0.01562 0.00000 0.00000

FISSIONS / ENERGY (WS):
3.04377E+10

11	12	14	12
1	12	15	12
2	12	16	12
3	12	17	12
4	12	18	12
5	12	19	12
6	12	20	12
7	12	21	12
8	12	22	12
9	12	23	12
10	12	24	12
13	12	12	12

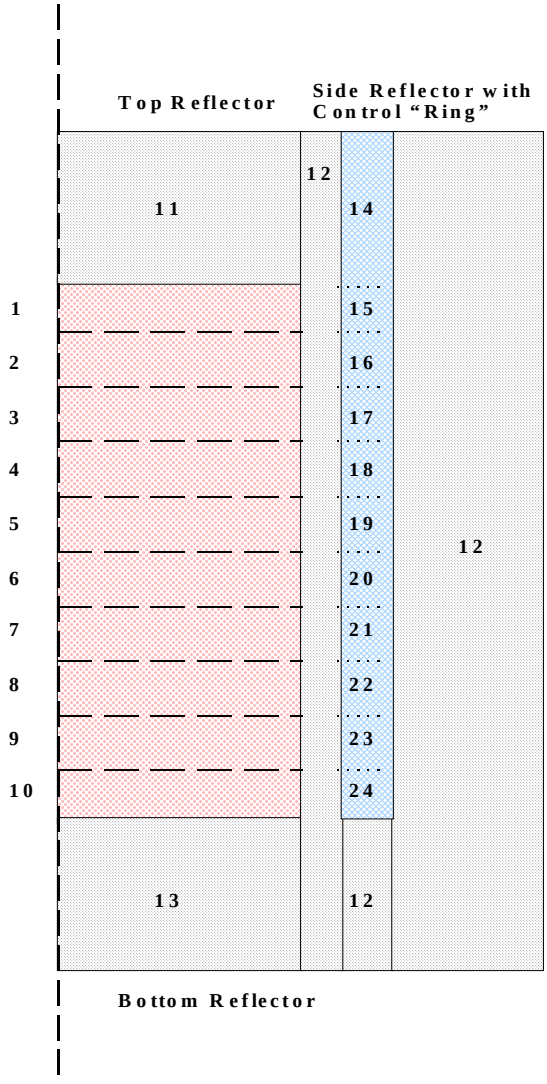

Figure 1. Geometry Description of Test Case 1

3.2 Geometric and Material Description of Test Case 2

Test case 2 is similar to test case 1 except for the step-wise insertion of control rods into the peripheral regions 14 to 24 as shown in Figure 1 below. It should be noted then, that the cross sections for layers 14 – 24 would vary as this stepwise insertion takes place. When all the rods are out it is herein referred to as All Rods Out (ARO) and when the rods are fully inserted it is referred to as All Rods In (ARI).

3.3 Geometric and Material Description of Test Case 3

Test case 3 is a more realistic model of equilibrium PBMR reactor core with a thermal power of 268 MWt. A bottom cone area, directing pebble flow to a central de-fueling chute, and a 10-pass fuel management system were introduced. A geometrical presentation of test case 3 is shown in Figure 2. Note that the cross-sections data sets used were however obtained from VSOP on the CITATION material mesh (R-Z), which implies that the flow speed variations and non vertical flow lines (due to the bottom cone) were already taken into account (by volume weighting and averaging) in the cross-section sets prepared. In this problem, there are 286 regions, and thus 286 cross section sets of which 225 of them are within the fuel region. The core is 350 cm wide and 850 cm high, with varying mesh sizes for both the axial and the radial directions. For the void regions multi-directional diffusion coefficients are provided in the specifications. Table 1 below shows the overall design parameters for the PBMR design used in test case 3. Table 2 shows the actual material specifications for the reflector regions for test case 3 and Figure 3 shows the actual material mesh for the test case 3. The calculational mesh is given in Table 3.

Table 1: Design Parameters for the 268MWth PBMR Core

Thermal Power (MW)	268
Core Diameter (m)	3.5
Core Height (m)	8.5
Mean Power Density (W/cc)	3.25
Diameter of Inner Reflector (m) with mixing zone	0.8m – 1.13m
Number of Pebbles (fuel/graphite)	330000 / 110000
System Pressure (MPa)	7.0
Helium Temperature (°C inlet/outlet)	530 / 900
Number of control rods	9 upper, 9 lower
Number of Absorber ball systems	17
Average No. of Passes per Pebble	10
No. of Particles per Pebble	15000
Heavy Metal Loading (g/pebble)	~9
Enrichment($\%U^{235}$)	~8.1
Fresh Fuel Injection Rate (pebbles/day)	~380
Discharge Burnup (MWD/kg)	80
Fuel Residence Time (days)	~850

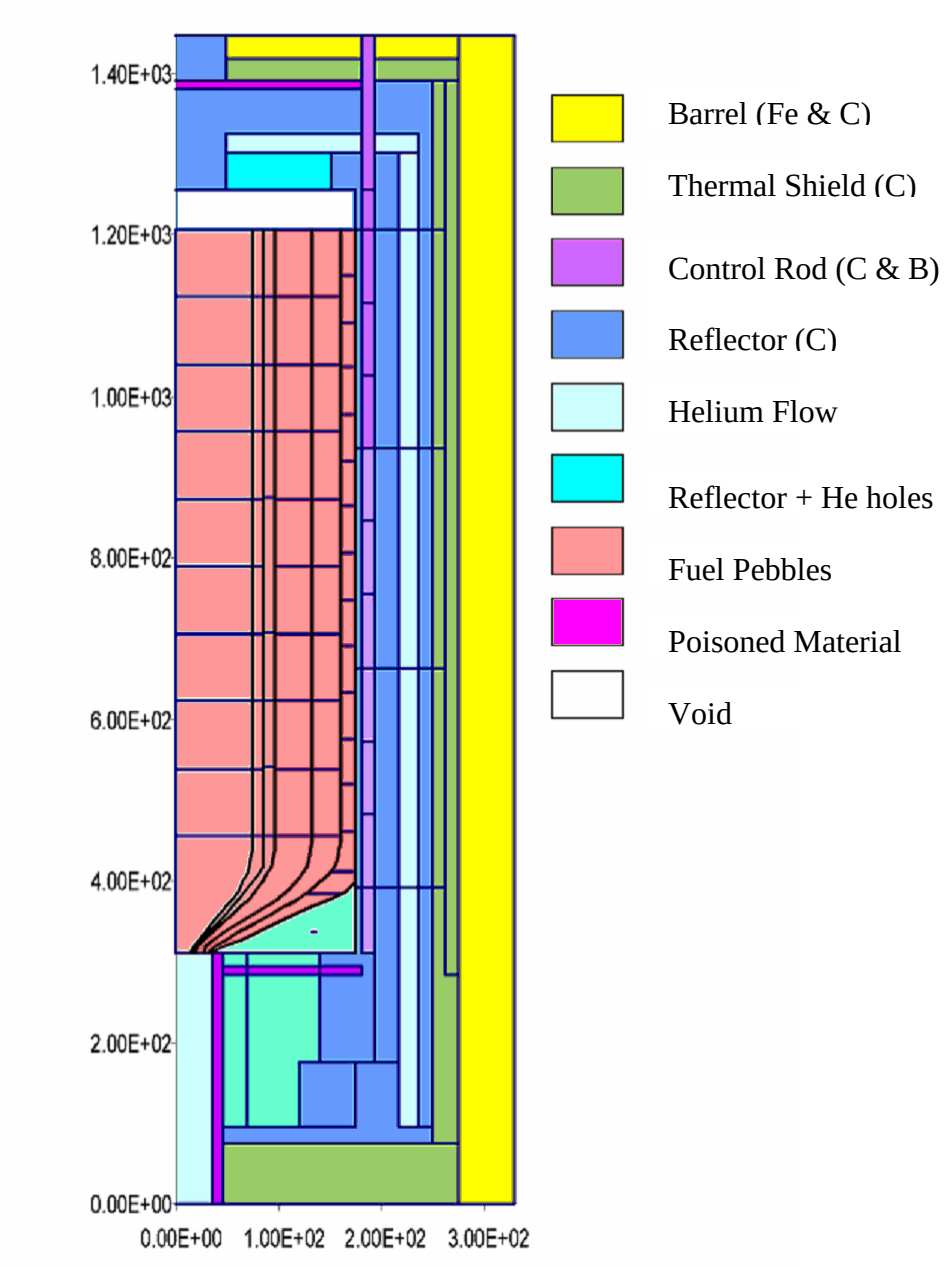

Figure 2: Geometric and Material Description of Test case 3

T	O	P						R	A	D	I	A	L						
	#		1	2	3	4	5	6	7	8	9	10	11	12	13	14	15	16	17
		Sizes	35	10	3	22	25	24.4	20.6	11	24	6	13	22.5	19	14.5	13.5	11.5	56
	1	30	279	279	279	282	282	282	282	282	282	282	241	283	283	283	283	283	274
	2	25	279	279	279	226	226	226	226	226	226	226	241	253	253	253	253	253	274
	3	11.5	278	278	278	278	278	278	278	278	278	278	241	265	265	265	269	286	274
	4	56	277	277	277	277	277	277	277	277	277	277	241	265	265	265	269	286	274
	5	22.5	277	277	277	227	227	227	227	227	227	227	241	254	254	265	269	286	274
	6	45	277	277	277	228	228	228	228	228	235	235	241	255	260	265	269	286	274
	7	50	229	229	229	229	229	229	229	229	229	235	242	255	260	265	269	286	274
	8	45.3	1	26	51	76	101	126	151	176	201	236	243	256	261	266	270	286	274
	9	45.3	2	27	52	77	102	127	152	177	202	236	243	256	261	266	270	286	274
	10	45.3	3	28	53	78	103	128	153	178	203	236	244	256	261	266	270	286	274
	11	45.3	4	29	54	79	104	129	154	179	204	236	244	256	261	266	270	286	274
	12	45.3	5	30	55	80	105	130	155	180	205	236	245	256	261	266	270	286	274
	13	45.3	6	31	56	81	106	131	156	181	206	236	245	256	261	266	270	286	274
	14	45.3	7	32	57	82	107	132	157	182	207	237	246	257	262	267	271	286	274
	15	45.3	8	33	58	83	108	133	158	183	208	237	246	257	262	267	271	286	274
	16	45.3	9	34	59	84	109	134	159	184	209	237	247	257	262	267	271	286	274
	17	45.3	10	35	60	85	110	135	160	185	210	237	247	257	262	267	271	286	274
	18	45.3	11	36	61	86	111	136	161	186	211	237	248	257	262	267	271	286	274
	19	45.3	12	37	62	87	112	137	162	187	212	237	248	257	262	267	271	286	274
	20	45.3	13	38	63	88	113	138	163	188	213	238	249	258	263	268	272	286	274
A	21	45.3	14	39	64	89	114	139	164	189	214	238	249	258	263	268	272	286	274
	22	45.3	15	40	65	90	115	140	165	190	215	238	250	258	263	268	272	286	274
X	23	45.3	16	41	66	91	116	141	166	191	216	238	250	258	263	268	272	286	274
	24	45.3	17	42	67	92	117	142	167	192	217	238	251	258	263	268	272	286	274
I	25	45.3	18	43	68	93	118	143	168	193	218	238	251	258	263	268	272	286	274
	26	13.85	19	44	69	94	119	144	169	194	219	239	252	259	264	259	273	286	274
A	27	6.35	20	45	70	95	120	145	170	195	220	239	252	259	264	259	273	286	274
	28	11.89	21	46	71	96	121	146	171	196	221	239	252	259	264	259	273	286	274
L	29	14.08	22	47	72	97	122	147	172	197	222	239	252	259	264	259	273	286	274
	30	14.42	23	48	73	98	123	148	173	198	223	239	252	259	264	259	273	286	274
	31	12.7	24	49	74	99	124	149	174	199	224	239	252	259	264	259	273	286	274
	32	7.51	25	50	75	100	125	150	175	200	225	239	252	259	264	259	273	286	274
	33	16	230	285	231	231	232	232	232	239	239	239	239	259	264	259	273	286	274
	34	11.5	230	285	275	275	276	276	276	284	284	284	239	259	264	259	273	286	274
	35	108.5	230	285	280	280	281	281	281	239	239	239	239	259	264	259	273	273	274
	36	80	230	285	280	280	281	281	233	233	233	240	240	240	264	259	273	273	274
	37	20	230	285	240	240	240	240	240	240	240	240	240	240	240	240	273	273	274
	38	75	230	285	234	234	234	234	234	234	234	234	234	234	234	234	234	234	274

Figure 3: Material Mesh and Material Numbers for Testcase 3 Model (Coarse Mesh)

Table 2: Material Specification for the Reflector regions in Testcase 3

Region numbers	Area	Material	Void	Effective density	Impurities
226, 234, 253, 269–273, 286	Thermal shield	Carbon	0%	1.8 gcm^{-3}	12 x A3-3
227, 254, 260-264	He flow area	Graphite	33.3%	1.067gcm^{-3}	A3-3
228, cone, 231, 232,	Reflector with some gas slits or holes	Graphite	10.0%	1.44gcm^{-3}	A3-3
229, 233, 235-240, 255-259, 265-268, 277	Reflector	Graphite	0%	1.6 gcm^{-3}	A3-3
230	Defueling tube (fuel ignored)	Graphite	33.3%	1.067gcm^{-3}	A3-3
241-252	Control rod	Graphite / boron	31.2%	1.1008 gcm^{-3}	A3-3
274	Barrel and void area	Iron / graphite	NA	3.789 gcm^{-3} / 0.0178 gcm^{-3}	None
275, 276, 278, 284, 285	Poisoned areas	Graphite / B_4C pins	NA	TBD	A3-3
282	Top reflector plate	Iron / graphite	NA	7.86 gcm^{-3}/ 0.0178 gcm^{-3}	None

Table 3: Fine Calculational Mesh: Sizes and Distances for Radial Dimensions (Core Centre Outwards) and Axial Dimensions (Top to Bottom).

Radial Mesh #	Accumulative radius	Mesh thickness	Axial Mesh #	Accumulative height	Mesh height	Axial Mesh #	Accumulative height	Mesh height
1	0	20.207	1	0	15	47	693	15.1
2	20.207	8.37	2	15	15	48	708.1	15.1
3	28.577	6.423	3	30	12.5	49	723.2	15.1
4	35	10	4	42.5	12.5	50	738.3	15.1
5	45	3	5	55	11.5	51	753.4	15.1
6	48	12.017	6	66.5	18.667	52	768.5	15.1
7	60.017	9.983	7	85.167	18.666	53	783.6	15.1
8	70	13.442	8	103.833	18.667	54	798.7	15.1
9	83.442	11.558	9	122.5	11.25	55	813.8	15.1
10	95	12.892	10	133.75	11.25	56	828.9	15.1
11	107.892	11.508	11	145	15	57	844	15.1
12	119.4	10.708	12	160	15	58	859.1	15.1
13	130.108	9.892	13	175	15	59	874.2	15.1
14	140	11	14	190	16.667	60	889.3	15.1
15	151	8.402	15	206.667	16.666	61	904.4	15.1
16	159.402	7.981	16	223.333	16.667	62	919.5	15.1
17	167.383	7.617	17	240	15.1	63	934.6	15.1
18	175	2.023	18	255.1	15.1	64	949.7	15.1
19	177.023	1.999	19	270.2	15.1	65	964.8	15.1
20	179.022	1.978	20	285.3	15.1	66	979.9	15.1

Radial Mesh #	Accumulative radius	Mesh thickness	Axial Mesh #	Accumulative height	Mesh height	Axial Mesh #	Accumulative height	Mesh height
21	181	6.613	21	300.4	15.1	67	995	15.1
22	187.613	6.387	22	315.5	15.1	68	1010.1	15.1
23	194	7.779	23	330.6	15.1	69	1025.2	15.1
24	201.779	7.49	24	345.7	15.1	70	1040.3	15.1
25	209.269	7.231	25	360.8	15.1	71	1055.4	13.85
26	216.5	6.513	26	375.9	15.1	72	1069.25	6.35
27	223.013	6.329	27	391	15.1	73	1075.6	11.89
28	229.342	6.158	28	406.1	15.1	74	1087.49	14.08
29	235.5	4.931	29	421.2	15.1	75	1101.57	14.42
30	240.431	4.831	30	436.3	15.1	76	1115.99	12.7
31	245.262	4.738	31	451.4	15.1	77	1128.69	7.51
32	250	6.839	32	466.5	15.1	78	1136.2	5.333
33	256.839	6.661	33	481.6	15.1	79	1141.533	5.334
34	263.5	5.811	34	496.7	15.1	80	1146.867	5.333
35	269.311	5.689	35	511.8	15.1	81	1152.2	11.5
36	275	15.016	36	526.9	15.1	82	1163.7	36.167
37	290.016	14.275	37	542	15.1	83	1199.867	36.166
38	304.291	13.635	38	557.1	15.1	84	1236.033	36.167
39	317.926	13.074	39	572.2	15.1	85	1272.2	26.667
	331		40	587.3	15.1	86	1298.867	26.666
			41	602.4	15.1	87	1325.533	26.667
			42	617.5	15.1	88	1352.2	10
			43	632.6	15.1	89	1362.2	10
			44	647.7	15.1	90	1372.2	37.5
			45	662.8	15.1	91	1409.7	37.5
			46	677.9	15.1	92	1447.2	

3.4 Requested Output

The output for the three-benchmark cases consists of both integral parameters and local distributions. The integral parameters requested are k-eff (for all test cases) and control rod worths (integral and differential for test case 2. The local distribution output is requested in material mesh (course-mesh) format and consists of:

(a) 1-D core axial power distribution;

(b) 2-D (r-z) power distribution;

(c) 1-D core group axial flux distribution;

(d) 2-D (r-z) group flux distribution.

4. BENCHMARK RESULTS

Each of the three test cases was analyzed with VSOP (as reference solution), NEM and PARCS. The results were compared and a summary of some of the results is shown in this paper. Table 4 shows the calculated k-eff values for test cases 1 and 3. It should be noted that for test case 1 the following mesh sizes was used in the VSOP calculation: in radial direction – 10 meshes each of 10cm; one mesh of 6cm; one mesh of 13cm; nine meshes of 9cm (total of 21); in axial direction – 10 meshes each of 10cm; 30 meshes each of 10.6cm; and 10 meshes each of 10cm. (total of 50). The NEM meshes are as follows: in radial direction from the center - 5 meshes each of 20 cm; 6 cm; 13 cm; 3 meshes each of 27 cm; in axial direction - 2 meshes each of 50 cm; 10 meshes each of 31.8 cm; and 2 meshes each 50 cm. The PARCS mesh sizes used in this calculation are 1 cm in radial direction and 1.5 cm in axial direction. Node size sensitivity studies have been performed with VSOP by increasing simultaneously numbers of radial and axial meshes (i.e. by reducing simultaneously the mesh sizes in radial and axial directions). The results are presented in Table 5 demonstrating improved agreement with PARCS and NEM while refining the mesh sizes in VSOP. For test case 3 NEM is using the calculational mesh, specified in Figure 3, while PARCS and VSOP are using fine mesh sizes of about 1cm in both axial and radial directions. Table 6 shows k-eff comparisons for test case 2 where control rods were inserted from the top in meshes 14, 14-15 etc up to 14-24 (ARO indicates all rods out). In addition mesh-size sensitivity studies have been also performed with NEM. The coarse mesh solution is the base calculations as described above and fine mesh indicates the sizes of nodes in both radial and axial directions are divided by two. The PARCS meshes are as specified above. In summary good agreement has been observed in the predicted integral results for all of the three cases.

Figure 4 show the comparisons of core averaged relative axial power distributions as predicted by the three codes for test case 1 (ARO) while Figure 5 shows the same comparison for test case 2 (ARI) . The code predictions agree well with maximum deviation of 3 % in the upper part of the core. The maximum deviation in 2-D (R-Z) normalized power comparisons is 0.6 %. Figure 6 shows the core average relative axial power comparison for the test case 3. The slight shift between NEM results on one side and PARC and VSOP predictions on the other side (which is also observed in group flux comparisons) is attributed to the difference in the detail of calculational mesh used and different methods utilized. Figure 7 shows the axial distributions of group fluxes while Figure 8 shows the 2-D (r-z) group flux 4 distribution for test case 3 as predicted by VSOP. The last two figures illustrate the type of output requested from the potential participants in this benchmark.

Table 4. Comparison of k-eff Predictions for Test Cases 1 and 3

CASE/CODE	VSOP	NEM	PARCS
Test Case 1	0.98761	0.99423	0.99277
Test Case 3	1.00122	1.00175	1.00124

Table 5. Node Size Sensitivity Studies for Test Case 1

Radial Meshes	Axial Meshes	k-eff
21	50	0.98767
38	86	0.98989
77	173	0.99017
145	211	0.99034

Table 6. Node Size Sensitivity Studies for Test Case 2

CASE/CR POSITION	NEM/Coarse Mesh	NEM/Fine Mesh	PARCS
ARO	0.99423	0.99406	0.99277
14	0.98088	0.98056	0.97894
15	0.96295	0.96253	0.96135
16	0.94278	0.94228	0.94119
17	0.92295	0.92242	0.92130
18	0.90465	0.90406	0.90283
19	0.88871	0.88801	0.88658
20	0.87616	0.87531	0.87364
21	0.86769	0.86682	0.86494
22	0.86312	0.86213	0.86014
23	0.86096	0.86000	0.85791
24	0.86008	0.85913	0.85704

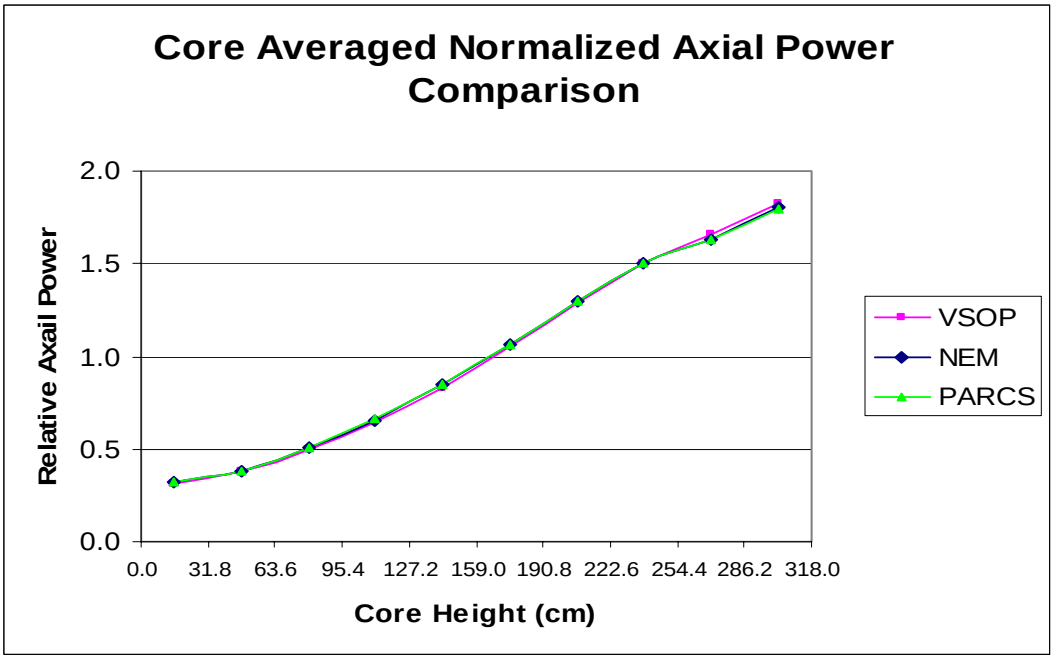

Figure4: Core Averaged Normalized Axial Power Comparisons (ARO)

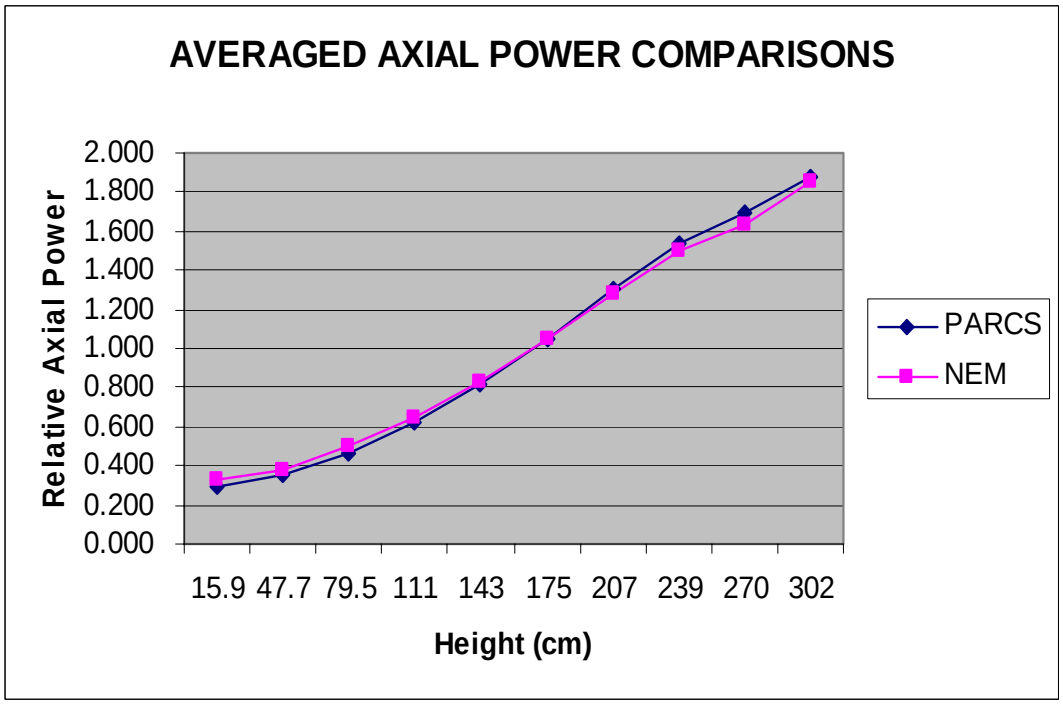

Figure 5: Core Averaged Normalized Axial Power Comparisons (ARI)

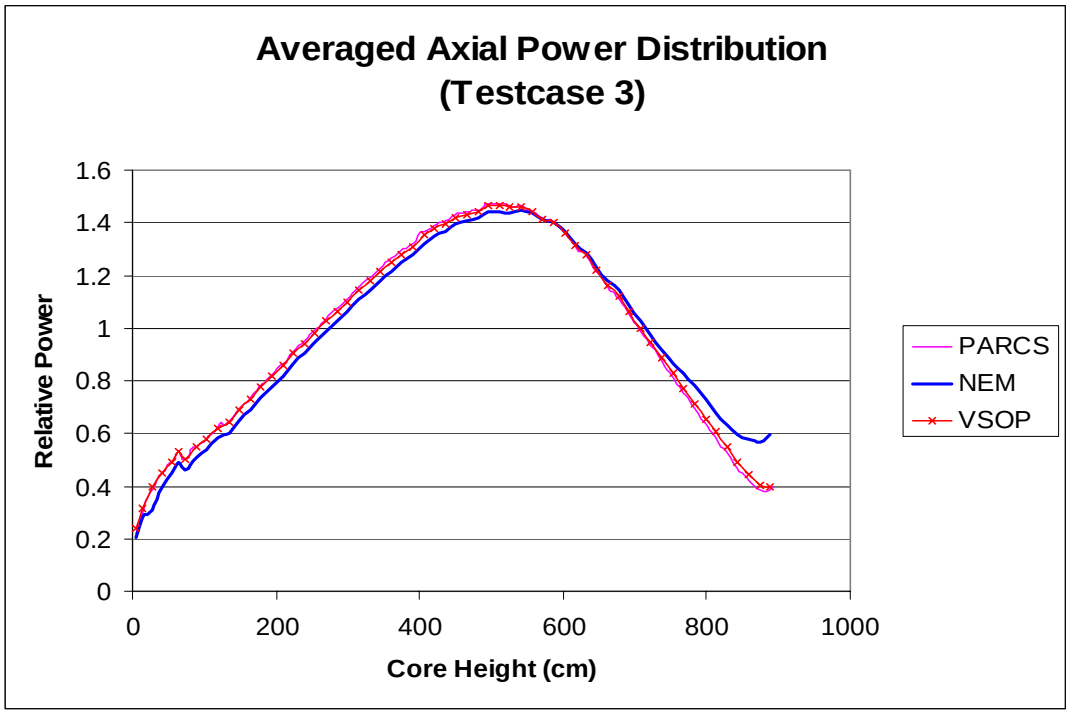

Figure 6: Core Averaged Normalized Axial Power Comparisons (Test Case 3)

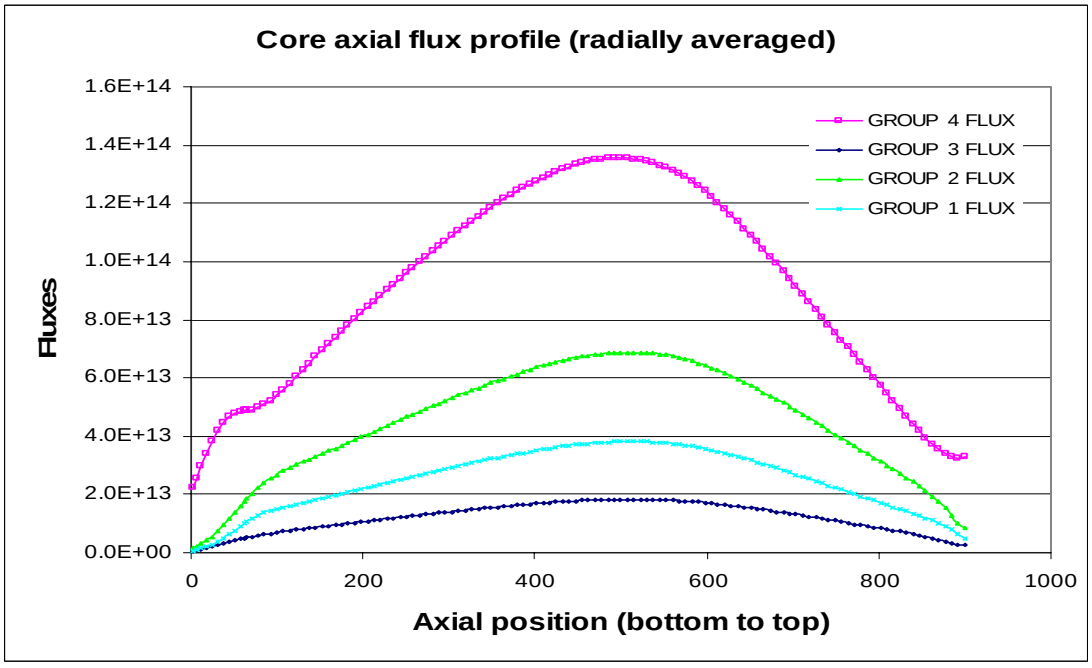

Figure 7. Axial Group Flux Distributions for Test Case 3 (VSOP Results)

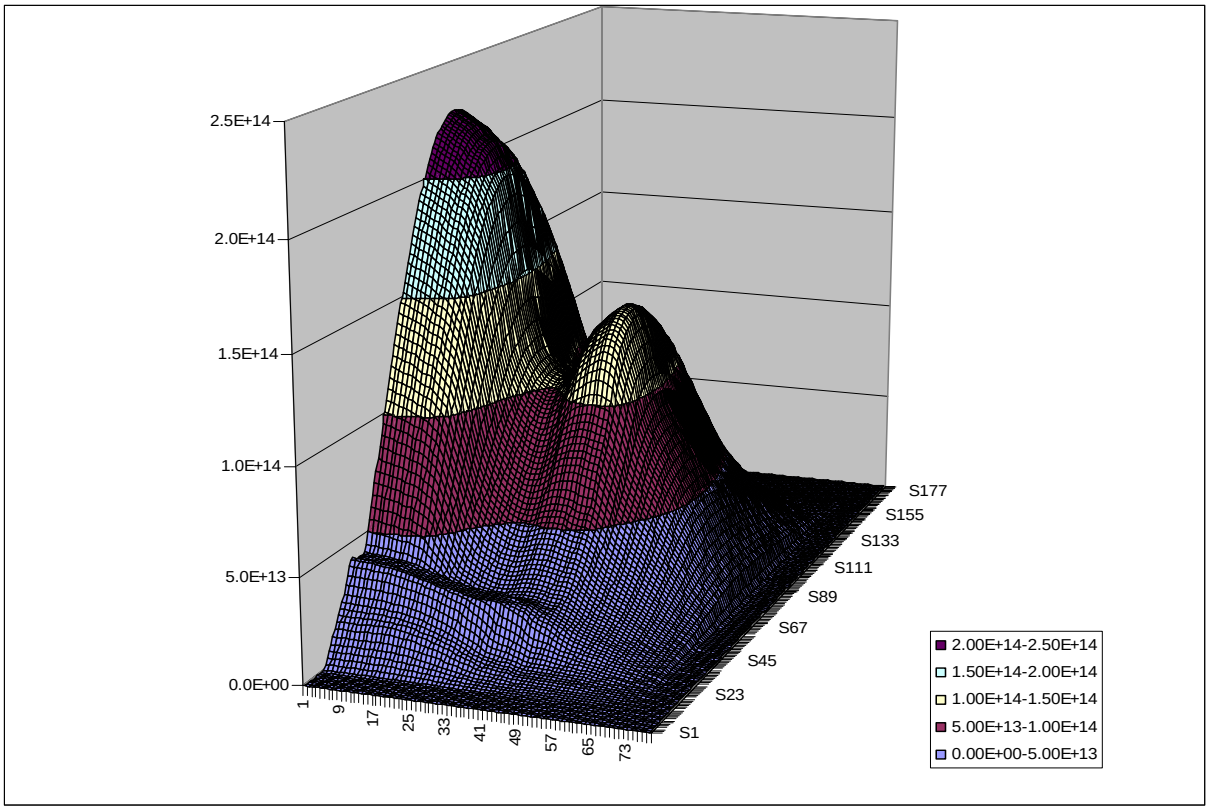

Figure 8. 2-D (r-z) Group 4 Flux Distribution - Test Case 3

3. CONCLUSIONS

Three PBMR core physics benchmark problems were defined for deterministic neutronics methods validation. The first two problems represent a simplified model of an HTGR operating on an once through then out (OTTO) fuelling scheme, whereas the third problem is a realistic 268 MWt PBMR core model operating on a multi-pass fuelling scheme. For each of the benchmark problems, four group cross sections and scattering matrices data are provided as a part of benchmark specifications. The development of this set of multi-dimensional computational test problems is a joint effort between three institutions namely: Penn State University, Purdue University and the PBMR Company in South Africa. The ultimate intention is to develop these test problems into HTGR benchmarks similar to the well-known IAEA PWR steady-state benchmarks]. The test cases developed here were analyzed with three different codes: VSOP (PBMR Co), NEM (Penn State), and PARCS (Purdue).

From the obtained results, (selected comparisons are shown in this paper) it is observed that a reasonable agreement between all the codes is obtained in terms of prediction of both integral parameters and local power and group flux distribution. Sensitivity studies are being performed to determine the effect of calculational mesh sizes in both axial and radial directions as well as the effect of modeling directional diffusion coefficients for the void regions. Results based on the diffusion theory will be also compared with the results produced with SP3 method implemented in PARCS in order to evaluate the necessity of using transport methods for PBMR core analysis.

ACKNOWLEDGMENTS

We would like to acknowledge the support of both the USNRC and the PBMR Company in South Africa in carrying out this work.

REFERENCES

1. "Argonne Code Center: Benchmark Problem Book", ANL-7416, Suppl. 2, ANL (1977).
2. Teuchert, E., Hansen, U., Haas, K., "VSOP – Computer Code System for Reactor Physics and Fuel Cycle Simulation," Kernforschunsanslage Jülich, JÜL-1649, March 1980
3. B. Tyobeka and K. Ivanov, "User Manual for Stand-alone 3-D NEM Core Simulator", The Pennsylvania State University, April, 2002.
4. H. Finnemann et al, "Interface Current Techniques for Multidimensional Reactor Calculations", *Atomkernenergie* (**30**), p123, (1977)
5. W. Scherer and H Gerwin, "Treatment of the upper cavity in the pebble-bed reactor, *Nuclear Science and Engineering*, **97**, 96-103 (1987)
6. H. Joo, D. Barber, R. Miller, T. Downar, "PARCS: A Multi-Dimensional Two-Group Reactor Kinetics Code Based on the Nonlinear Analytic Nodal Method" PU/NE-98-26, Purdue University, 1998.
7. F. Reitsma, B. Tyobeka, and K. Ivanov, "PBMR Core Physics Benchmarks – Final Specification", PBMR Ltd./PSU, March, 2002.